Effect of the chirality of the glycerol backbone on the bilayer and nonbilayer phase transitions in the diastereomers of di-dodecyl-β-D-glucopyranosyl glycerol

D. A. Mannock,* R. N. A. H. Lewis,* R. N. McElhaney,* M. Akiyama,‡ H. Yamada,‡ D. C. Turner,§ and S. M. Gruner§

*Department of Biochemistry, University of Alberta, Edmonton, Alberta, Canada, T6G 2H7; ‡Department of Physics, Sapporo Medical College, S.1, W.17, Chuo-Ku, Sapporo 060, Japan; and §Department of Physics, Joseph Henry Laboratories, Jadwin Hall, Princeton University, Princeton, New Jersey 08544, USA

ABSTRACT We have studied the physical properties of aqueous dispersions of 1,2-*sn*- and 2,3-*sn*-didodecyl-β-D-glucopyranosyl glycerols, as well as their diastereomeric mixture, using differential scanning calorimetry and low angle x-ray diffraction. Upon heating, both the chiral lipids and the diastereomeric mixture exhibit characteristically energetic L_β/L_α phase transitions at 31.7–32.8°C and two or three weakly energetic thermal events between 49°C and 89°C. In the diastereomeric mixture and the 1,2-*sn* glycerol derivative, these higher temperature endotherms correspond to the formation of, and interconversions between, several nonlamellar structures and have been assigned to L_α/Q_{II}^a, Q_{II}^a/Q_{II}^b, and Q_{II}^b/H_{II} phase transitions, respectively. The cubic phases Q_{II}^a and Q_{II}^b, whose cell lattice parameters are strongly temperature dependent, can be identified as belonging to space groups Ia3d and Pn3m/Pn3, respectively. In the equivalent 2,3-*sn* glucolipid, the Q_{II}^a phase is not observed and only two transitions are seen at 49°C and 77°C, which are identified as L_α/Q_{II}^b and Q_{II}^b/H_{II} phase transitions, respectively. These phase transitions temperatures are some 10°C lower than those of the corresponding phase transitions observed in the diastereomeric mixture and the 1,2-*sn* glycerol derivative.

On cooling, all three lipids exhibit a minor higher temperature exothermic event, which can be assigned to a H_{II}/Q_{II}^b phase transition. An exothermic L_α/L_β phase transition is observed at 30–31°C. A shoulder is sometimes discernible on the high temperature side of the L_α/L_β event, which may originate from a Q_{II}^b/L_α phase transition prior to the freezing of the hydrocarbon chains. None of the lipids show evidence of a Q_{II}^a phase on cooling. No additional exothermic transitions are observed on further cooling to −3°C. However, after nucleation at 0°C followed by a short period of annealing at 22°C, the 1,2-*sn* glucolipid forms an L_c phase that converts to an L_α phase at 39.5°C on heating. Neither the diastereomeric mixture nor the 2,3-*sn* glycerol derivative shows such behavior even after extended periods of annealing.

Our results suggest that the differences in the phase behavior of these glycolipid isomers may not be attributable to headgroup size per se, but rather to differences in the stereochemistry of the lipid polar/apolar interfacial region, which consequently effects hydrogen-bonding, hydration, and the hydrophilic/hydrophobic balance.

INTRODUCTION

Most studies of the thermotropic phase behavior of aqueous dispersions of membrane lipids have dealt with the 1,2-diacylphosphatides, particularly the phosphatidylcholines (PCs)[1] (1–8) and phosphatidylethanolamines (PEs) (5, 9–17), which are known to occur naturally in a wide range of eukaryotic cells (18). Although the effect of varying the length and structure of the hydrocarbon chain and the structure of the polar headgroup has been extensively investigated (1–4, 19), studies on the effect of variations in the stereochemical conformation of these glycerophospholipids on their thermotropic phase behavior are less common. While it has been established that there are marked differences in the lamellar gel-state polymorphism of the 1,2-*sn* (L) isomers and the racemic (DL) mixtures of both dipalmitoylphosphatidylcholine (DPPC) (2, 5–8, 20) and dipalmitoylphosphatidylethanolamine (DPPE) (5, 9–13, 17, 21), there have been very few studies of the lamellar phases of the 1,2-*sn* and 2,3-*sn* isomers (22), which are often assumed to exhibit identical physical properties. Even though this has not been verified experimentally, it seems a reasonable assumption, since these phospholipid molecules contain only a single chiral center (at C2 of glycerol) and thus the 1,2-*sn*- and 2,3-*sn* isomers are mirror images (enantiomers). However, this assumption is not valid for lipids with more than one chiral center, where the 1,2-*sn*- and 2,3-*sn*-glycerol isomers are diastereomers instead of enantiomers. Indeed, the introduction of a second chiral center at phosphorus by replacing an oxygen with a sulfur atom produces diastereomers of PC that differ significantly in the physical properties of their lamellar phases (23, 24). Similar differences in gel-phase polymorphism have also been

Address correspondence to Dr. Mannock.

Dr. Turner's current address is Center for Biomolecular Science and Engineering, Code 6090, Naval Research Laboratory, Washington, DC 20375.

[1] Abbreviations used in this paper: PC, phosphatidylcholine; PE, phosphatidylethanolamine; PG, phosphatidylglycerol; PS, phosphatidylserine; DPPC, dipalmitoylphosphatidylcholine; DPPE, dipalmitoylphosphatidylethanolamine; DHPE, dihexadecylphosphatidylethanolamine; DOPE, dioleoylphosphatidylethanolamine; DDPE, didodecylphosphatidylethanolamine; SPM, sphingomyelin; β-GalDAG, β-D-galactopyranosyl dialkylglycerol; β-GlcDAG, β-D-glucopyranosyl dialkylglycerol; DD-β-GlcDAG, didodecyl-β-D-glucopyranosyl glycerol; β-GlcDG, β-D-glucopyranosyl diacylglycerol; DSC, differential scanning calorimetry; NMR, nuclear magnetic resonance spectroscopy; T_m, transition temperature.

0006-3495/92/11/1355/14 $2.00

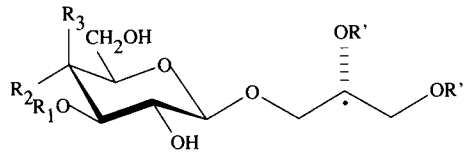

FIGURE 1 The chemical structure of di-dodecyl-β-D-glucosyl glycerols used in this study. R_1 = H, R_2 = OH, R_3 = H, R' = dodecyl. The dot denotes the chiral center of the glycerol moiety.

observed for the diastereomeric (D-*erythro* and L-*threo*) forms of sphingomyelin (25, 26). However, neither of these lipids forms a nonlamellar structure.

Until recently, it was not known if the structures of the nonlamellar phases of PEs were dependent on the chirality of the glycerol backbone, but the latest measurements of 1,2-*sn* and racemic dimethyl dihexadecylphosphatidylethanolamine (DHPE) at low water content were unable to detect differences in either the structure or dimensions of the cubic phase formed (27). To date, however, there have been no studies of the physical properties of diastereomeric thio-PEs similar to those of the thio-PCs (23, 24). Thus, with glyceroglycolipids, which are known to form both lamellar and nonlamellar structures, the addition of a chiral center at C5 of each sugar molecule might be expected to produce differences in the physical properties of the 1,2-*sn* and 2,3-*sn* glycerol isomers. However, so far the biophysical studies of the dialkyl glycolipids have concentrated on a small number of 1,2-di-*O*-alkyl-3-*O*-(β-D-glucopyranosyl)- (28–32) and -(β-D-galactopyranosyl)-*sn*-glycerols (33) and a few impure diastereomeric mixtures (34, 35), and have not investigated the properties of the naturally occurring 2,3-*sn* stereoisomers.

In view of the widespread occurrence of 1,2-*sn* and 2,3-*sn* glycoglycerolipids in higher plant and eubacterial and archaebacterial membranes, respectively (36, 37, and references cited therein), we have embarked on a program to synthesize (38, 39) and investigate the thermotropic properties of a range of glycosyl dialkyl glycerols. Our studies of the phase behavior of these compounds have concentrated on the pattern of both gel-phase and nonlamellar-phase polymorphism in relation to the anomeric configuration of the glycoside bond (40–42), the stereochemistry of the hexopyranose ring (40, 43), and the nature of the linkage between the hydrocarbon chains and the glycerol backbone (44). Here, we present a detailed calorimetric and low angle x-ray diffraction study of two di-dodecyl-β-D-glucopyranosyl dialkylglycerols differing only in their chirality at C2 of the glycerol moiety and of their diastereomeric mixture.

MATERIALS AND METHODS

The general chemical structure of the lipids used in this study is shown in Fig. 1. Details of the synthesis and purification of these compounds have been described elsewhere (44). The hydrocarbon chain homogeneity and lipid purity were at least 99% as judged by gas-liquid and thin-layer chromatography, respectively. ^{1}H-NMR spectroscopy of the peracetates showed an anomeric ratio (β/α) of ~20:1.

Differential scanning calorimetry (DSC) was performed using a DSC-2C device (Perkin-Elmer Corp., Norwalk, CT) equipped with a 3700 data station using TADS software and other programs developed in this laboratory. Lipid samples were prepared in stainless-steel, large-volume capsules by heating the capsule containing a small aliquot (3–4 mg) of lyophilized lipid to a temperature above that of its softening point on a hot stage. 50 μl of distilled water were then added, and the capsule sealed and repeatedly heated and cooled between −3°C and 97°C to ensure thorough hydration of the contents. Repeated heating and cooling accelerates the convergence of the transition temperatures and d-spacings to constant values. Crossing phase boundaries facilitates this by reorganizing the lipid and water. The lipids were quantified by gas chromatography and the enthalpy values were calculated as described earlier (44).

Samples for x-ray diffraction were prepared by transferring 3–5 mg of dry lipid into a thin-walled glass capillary (1.5 mm). Deionized water (1–2 times the dry lipid weight) was added and the capillaries were either flame sealed or sealed with 5-min epoxy. The samples were mixed by repeatedly heating and cooling the capillaries with a hot air gun and by centrifuging the material back and forth in the capillary. The samples were determined to be uniformly dispersed when different parts of the x-ray capillary all yielded the same diffraction. The x-ray diffraction experiments were performed over the range −20 to 90°C.

Two generator-based low angle x-ray systems were employed. The first system (Princeton, NJ) consisted of a RU200 rotating anode generator (Rigaku/USA Inc., Danvers, MA), which was focused to give a 0.2 mm × 0.4 mm beam at the sample. The two-dimensional low angle scattering patterns were recorded using the Princeton SIT detector (45). The temperature of the sample was controlled with a precision of ±0.5°C by a thermoelectrically controlled sample stage. Data was collected at 10, 5, or 2°C intervals after the sample had been equilibrated for 10 min. Typical exposure times for each measurement were of the order of 2 min.

The second system (Sapporo, Japan) was attached to a Rigaku RU200 rotating anode generator and used a linear 512-channel, 28.3 mm metal oxide semiconductor multichannel photodiode to detect the low angle scattering patterns, which were then digitally recorded on a computer (46). The sample temperature was regulated by means of a sample holder connected to a circulating bath, the temperature of which was controlled by a computer with a precision similar to that reported above. Measurements were taken at approximately 2–3°C intervals after a 5–10 min equilibration period. Exposure times were typically of the order of 10 min.

Some experiments were conducted using synchrotron orbital radiation at station BL-15A, KEK, Tsukuba, Japan. The x-ray patterns were detected using a position-sensitive proportional counter and recorded digitally on a DEC computer. The temperature control system was similar to that reported above. The heating and cooling rates employed were of the order of 0.5°C min^{-1} with exposure times of about 30 s. A typical heating experiment over a temperature range of 10° took ~20 min.

RESULTS

Calorimetry studies. Illustrated in Fig. 2 are DSC thermograms of (*A*) the 1,2-di-dodecyl-(β-D-glucopyranosyl)-*sn*-glycerol, (*B*) the diasteromeric mixture and (*C*) the 2-3-di-dodecyl-(β-D-glucopyranosyl)-*sn*-glycerol. All three samples show a similar but complex pattern of phase behavior on heating, consisting of at least three endothermic events. The more energetic, lower temperature event has been assigned to a lamellar gel (L_β)/lamel-

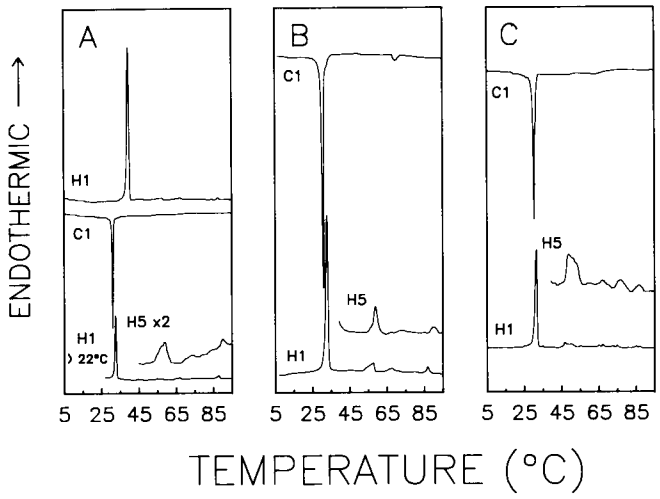

FIGURE 2 DSC thermograms of: (*A*) 1,2-*sn*-, (*B*) 1,2-*rac*-, and (*C*) 2,3-*sn*-di-dodecyl-(β-D-glucopyranosyl) glycerols. The heating (*H*) and cooling (*C*) rates are given in °C. The baseline aberrations in *C* are noise and do not show corresponding events in the x-ray diffraction experiments.

lar liquid crystalline (L_α) phase transition, whereas the less energetic, higher temperature events can be assigned to L_α/cubic (Q_{II}) and Q_{II}/inverted hexagonal (H_{II}) phase transitions, respectively. The L_β/L_α phase transition temperatures in all three compounds are very similar (31.7–32.8°C), as are the corresponding enthalpies (Table 1). A comparison of the less energetic phase transitions found at higher temperatures in all three lipids shows that those seen in the diastereomeric mixture and the 1,2-*sn* stereoisomer also occur at similar temperatures. However, those of the 2,3-*sn* stereoisomer show a slightly different pattern and occur at noticeably lower temperatures, specifically 58 and 88°C (diastereomeric mixture and 1,2-*sn*) versus 50 and 77°C (2,3-*sn*). Upon cooling, all three lipids show similar DSC curves, consisting of a weakly energetic, higher temperature exothermic event, which may correspond to a H_{II}/Q_{II} phase transition, and a more energetic, lower temperature exotherm, which corresponds to the L_β/L_α phase transition seen on heating. In addition at fast scan rates, a small shoulder is sometimes visible on the high temperature side of the major cooling exotherm, which probably originates from a Q_{II}/L_α phase transition. This assignment seems plausible because the x-ray patterns seem to show coexistence of the L_α and Pn3m/Pn3 cubic phases at those temperatures.

In the case of the 1,2-*sn* diastereomer, thermograms obtained at heating rates of up to $10°C \cdot min^{-1}$ show evidence of a second gel phase, which is visible as a very energetic endothermic event at a temperature between the L_β/L_α and the L_α/Q_{II} phase transitions. Such behavior is characteristic of the melting of highly ordered, crystal-like gel (L_c) phases and the endothermic event seen at 39.5°C can be tentatively assigned to an L_c/L_α phase transition. Formation of the L_c phase from the L_β phase was extremely rapid in samples which had been cooled to low temperature. Thus, in order to obtain the pure L_β phase in this compound, it was necessary to cool the sample only to 22°C, to avoid nucleation of the L_c phase, and to reheat the sample immediately. Samples of the 2,3-*sn* stereoisomer and the diastereomeric mixture, nucleated at −3°C and subsequently annealed for long periods of time at either 4°C or 22°C, show no evidence of gel-phase polymorphism. Since the tendency to form stable gel phases is known to be chain-length dependent (2, 40, 41), we investigated other members of the 2,3-*sn*- or 1,2-*rac*-β-GlcDAG series to see if L_c phases were formed on prolonged incubation. However, under our conditions not even the shortest members of these series (with a chain length of 10 carbon atoms) formed an L_c phase even after storage for some 3 yr at 4°C.

X-ray diffraction studies. X-ray diffraction measurements of these lipids over a wide range of temperature have enabled us to identify the structural nature of the thermal events seen by DSC. Diffraction patterns with intensity profiles characteristic of L_β, L_α, cubic, and H_{II} phases were observed in all three lipids. As shown in Fig. 3, the transition temperatures of the events measured by x-ray diffraction are in good agreement with those measured by calorimetry and they can be attributed to L_β/L_α (~32°C), L_α/Q_{II} (49–59°C), and Q_{II}/H_{II} (77–89°C) phase transitions, respectively. The lamellar phases showed low angle reflections in the ratios 1, 2, 3, and 4. Reflections 1 and 4 were visible in the L_β phase and 1, 2, and 3 in the L_α phase. In any case, at least two peaks were used for fitting. Typical lattice repeat vectors **a** (nm, ±0.05 nm) for the lamellar phases of the 1,2-*sn* compound were as follows: 5.15 nm (L_β at 0°C), 4.70 nm (L_α at 40°C). The 1,2-*sn* diastereomer also shows a diffraction pattern characteristic of a highly ordered L_c-type phase with a first-order spacing of 4.8 ± 0.3 nm.

At high temperatures in all three compounds, two minor thermal events are observed by DSC corresponding to sharp changes in the x-ray diffraction pattern, herein noted as L_α/Q_{II} and Q_{II}/H_{II} phase transitions. The samples typically yielded only three to five sharp orders of diffraction. The degree of confidence one has in a lattice assignment is very much a function of the number of orders observed and the type of lattice in question. Thus, 3–5 orders in the relative distance ratios 1, 2, 3, 4, 5 · · ·, and with a unit cell size similar to that typically observed with other fully hydrated lipids, indicate a lamellar lattice with a high degree of confidence. In conjunction with the DSC, this may be assigned to a L_β/L_α phase transition. Likewise, reflections in the ratios of 1, $\sqrt{3}$, 2, $\sqrt{7}$, 3 · · ·, and with the observed values of the basis vector length **a** (e.g., 5.62 nm ± 0.05 nm at 80°C, seen for the 1,2-*sn* compound on cooling) is highly suggestive of a hexagonal lattice; the fact that the lattice spacing doesn't swell above certain full hydration limits

TABLE 1 **Phase transition temperature (T_m, °C) and enthalpy (ΔH, Kcal/mol) values for the stereoisomers of various phospho- and glycolipids**

	L_c/L_α		L_c/L_β		$P_{\beta'}/L_\alpha$		L_β/L_α		L_α/Q_{II}		Q_{II}/H_{II}		L_α/H_{II}	
Lipid species	T_m	ΔH	T_m	ΔH	T_m	ΔH	T_m	ΔH	T_m	ΔH	T_m	ΔH	T_m	ΔH
β-GlcDAG [28, 44]														
12:0-1,2-*sn*	39.5	15.1	—	—	—	—	32.5	4.55	58.2	0.48*	88.5	0.14	—	—
12:0-1,2-*rac*	—	—	—	—	—	—	32.8	4.37	56.8	0.46*	86.7	0.19	—	—
12:0-2,3-*sn*	—	—	—	—	—	—	31.7	4.47	49.9	0.52*	77.0	0.15	—	—
14:0-1,2-*sn*	52.1	—	50.1	—	—	—	51.9	—	—	—	—	—	57.3	—
	—	—	—	—	—	—	50.8	5.9	—	—	—	—	56.9	1.2
14:0-1,2-*rac*	—	—	—	—	—	—	51.9	—	—	—	—	—	56.8	—
14:0-2,3-*sn*	—	—	—	—	—	—	51.9	—	—	—	—	—	57.0	—
β-GalDAG [this work, 33, 48]														
12:0-1,2-*sn*	58.2	10.8		—	—	—	31.7	0.3‡	—	—	—	—	—	—
12:0-1,2-*rac*	53.0	—	44.4	—	—	—	32.9	—	66.7	—	—	—	—	—
14:0-1,2-*sn*	69.3§	—	—	—	—	—	52.6	—	—	—	—	—	64.7	—
	68.9	17.8	—	—	—	—	52.7	0.6‡	—	—	—	—	—	—
14:0-1,2-*rac*	54.7	—	60.8	—	—	—	52.0	—	—	—	—	—	63.1	—
14:0-2,3-*sn*	56.0	—	—	—	—	—	52.0	—	—	—	—	—	63.1	—
Di-myristoyl-glycosyl-glycerols														
1,2-β-Glc [40]	46.5	18.3	—	—	—	—	45.5	6.7	72.0	0.8	—	—	—	—
1,2-β-Gal [43]	75.4	20.7	—	—	—	—	48.7	6.8	80.6	0.4	—	—	—	—
1,2-α-Glc [41]	58.2	21.2	—	—	—	—	40.5	7.4	105.0	0.3	—	—	—	—
Phospholipids														
L-DPPC [2, 7]	—	—	17.6	3.3	40.7	8.8	—	—	—	—	—	—	—	—
	—	—	21.2	6.2	41.4	7.7	—	—	—	—	—	—	—	—
DL-DPPC [7]	—	—	—	—	40.8	8.7	—	—	—	—	—	—	—	—
L-DPPE [10, 12, 13, 15]	65.3	21.2	—	—	—	—	62.2	9.6	—	—	—	—	123.0	0.3
	64.9	18.5	—	—	—	—	63.2	8.8	—	—	—	—	—	—
	—	—	—	—	—	—	64.0	7.9	—	—	—	—	—	—
DL-DPPE [13]	81.7	20.5	—	—	—	—	60.9	8.7	—	—	—	—	—	—
L-DDPE [10, 11, 27]	44.0	—	—	—	—	—	35.0	3.8	~86.0	—	135.0	—	—	—
D-SPM [25]	—	—	36.0	5.7	—	—	44.7	6.8	—	—	—	—	—	—
	—	—	33.4	2.6	—	—	—	—	—	—	—	—	—	—
	—	—	43.6	8.0	—	—	—	—	—	—	—	—	—	—
DL-SPM [25]	—	—	—	—	—	—	44.0	7.5	—	—	—	—	—	—
L-SPM [25]	—	—	43.1	1.9	—	—	44.2	6.0	—	—	—	—	—	—
	—	—	35.0	6.0	—	—	—	—	—	—	—	—	—	—

* The ΔH values for the L_α/Q_{II} phase transitions presented here were obtained from 5°C/min^{-1} heating scans. The values obtained at 1°C/min^{-1} were approximately 50% lower than those shown above, but the width of the transitions made consistent measurements extremely difficult.
‡ These values are low because of the fast conversion from the L_β phase to the L_c phase.
§ This event is an L_c/H_{II} phase transition.

strongly suggests that the lattice is of the inverse, H_{II} type. This is supported by the DSC, the chemical structure of the lipid and diffraction studies of chemically similar lipids (33, 40–44, 47).

The lattice assignments for the Q_{II} phase are subject to more uncertainty than the L_α or H_{II} phase assignments because a larger number of x-ray reflections are needed to unambiguously distinguish between the various types of three-dimensionally periodic lattices. For example, the Q_{II} phase seen in the DD-β-GlcDAGs at ~65°C yields reflections in the ratio $\sqrt{3}$, 2, $\sqrt{6}$, $\sqrt{8}$, 3 · · ·, and a lattice repeat vector **a** of 8.09 nm ± 0.05 nm (the 1,2-*sn* compound measured at 70°) is consistent with either the Pn3m or Pn3 cubic lattices. We tentatively choose the Pn3m/Pn3 assignment because the lattice dimensions appear to be consistent with the Pn3m/Pn3 values observed with studies of other lipids, where more reflections are available (16, 27, 48). We note that there are too few diffracted orders for a definitive lattice assignment because the cubic phases seen in our study were indexed using between three and five reflections. Above 77°C (2,3-*sn*) or 88°C (1,2-*rac* and 1,2-*sn*), the Pn3m cubic phase is transformed into a H_{II} phase, which was indexed as described above using at least three reflections.

Upon increasing the temperature, the d-spacings of the L_β phase remain almost constant and are virtually identical in all three compounds. Those of the corresponding L_α and H_{II} phases decrease slightly with increasing temperature, as has been observed for the H_{II} phase of DOPE (49), but show no dependence on the stereochemistry of the glycerol backbone. The dimensions of the cubic phases of these DD-β-GlcDAGs and their diastereomeric mixture are strongly temperature

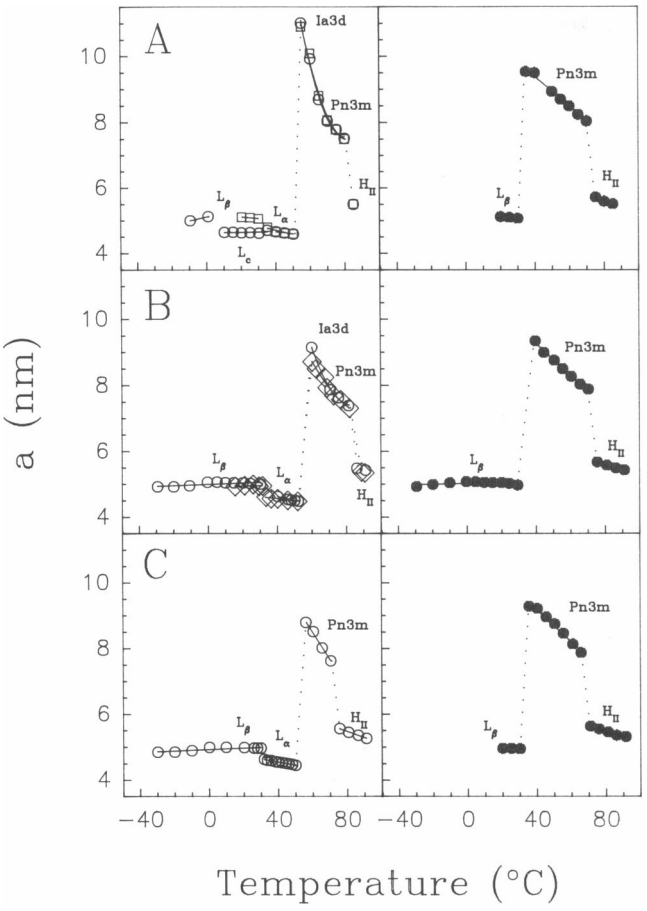

FIGURE 3 Plots of the cell lattice parameter, **a** (nm) as a function of temperature (°C) for the (*A*) 1,2-*sn*-, (*B*) 1,2-*rac*- and (*C*) 2,3-*sn*-didodecyl-(β-D-glucopyranosyl) glycerols. In the entire diagram, measurements denoted by circles and squares were performed at Princeton. The empty circles and squares indicate the first and second heating measurements, respectively, whereas the filled circles are data collected in the cooling mode. The empty diamonds denote heating measurements made in Sapporo. The dotted lines mark the transitions between phases and are merely a guide to the eye.

dependent. A comparison of the region close to the L_α/Q_{II} phase transition in these samples shows a considerable discrepancy between the magnitude of the cell lattice parameter **a** (nm) measured in the heating and cooling modes. Although the values of **a** for the cubic phases of all three samples are similar on cooling, the corresponding heating measurements obtained for both the 1,2-*sn* diastereomer and the diastereomeric mixture are significantly larger and show a greater decrease as the temperature increases. The corresponding heating and cooling measurements in the cubic phase region of the 2,3-*sn* diastereomer are almost identical. Thus, the magnitude of these differences in cubic phase d-spacings changes with the chirality of the glycerol moiety, being greatest in the 1,2-*sn*- diastereomer and least in the 2,3-*sn*- diastereomer.

The diffraction patterns observed at higher temperatures on heating in all three samples are consistent with a cubic phase belonging to the Pn3m/Pn3 space group. At temperatures close to the L_α/Q_{II} phase transition in the heating mode there is some disorder in the cubic phase diffraction patterns and the indexing is less reliable. A possible explanation for this is that the number of cubic phases observed on heating above the L_α/Q_{II} phase transition is dependent on the chirality of the glycerol backbone and that more cubic phases are present on heating than are seen on cooling. This seems plausible if one considers that it may not be possible to isolate each cubic phase in the heating experiment, because of the relatively large temperature intervals and long exposure times necessary when using a generator as the x-ray source. Such conditions are more likely to favor the capture of a diffraction pattern originating from a mixed cubic phase, when the two transitions are close together and neither is highly cooperative. This hypothesis is consistent with the pattern of the minor endothermic events seen in the DSC traces between 50° and 90°C on heating, and in their absence on cooling in all three lipids.

To investigate the possible existence of additional cubic phases, some samples of the diastereomeric mixture were examined using synchrotron radiation. Stacked plots of diffraction patterns obtained from a typical series of heating and cooling measurements, in which the temperature profile of the sample was changed linearly at $0.5°C \cdot min^{-1}$, are shown in Fig. 4. The diffraction patterns obtained on heating (Fig. 4 *A* and *C*) show a sudden change in the d-spacing at the L_β/L_α phase transition from 5.05 nm (at 29.9°C) to 4.69 nm (at 34.8°C). On further heating to 50°C, the L_α phase shows a gradual conversion to a cubic phase with a cell lattice parameter (**a**) of 8.93 nm (at 57.4°C); the structure of this cubic phase has not been unambiguously identified at the present time, but the 3–5 reflections are not consistent with the L_α, H_{II}, or Pn3m/Pn3 lattices. Rather the spacing ratios follow $\sqrt{6}$, $\sqrt{8}$, $\sqrt{14}$, $\sqrt{4}$, $\sqrt{20}\cdots$, as expected from an Ia3d (gyroid) space group. Continued heating to ~64°C results in a transition from the first cubic phase to the Pn3m/Pn3 cubic phase, which has slightly smaller lattice dimensions (8.06 nm at 69.9°C). Interestingly, the measurements of the 1,2-*sn* compound performed on the generator system in Princeton show a temperature window in the cubic phase region where these two cubic phases coexist. The width of this window may be larger than that seen in the diastereomeric mixture and we are attempting to perform some synchrotron measurements on the 1,2-*sn* compound to confirm this observation. The total absence of an Ia3d-like cubic phase in the 2,3-*sn* diastereomer suggests that the mechanism or kinetics of the conversion of the L_α to the Pn3m cubic phase may be different in each case. This is supported by measurements performed on the synchrotron line at faster heating rates ($1°C \cdot min^{-1}$) (Akiyama, M., unpublished observations), which show the existence of an additional phase in the diastereomeric mixture, which we

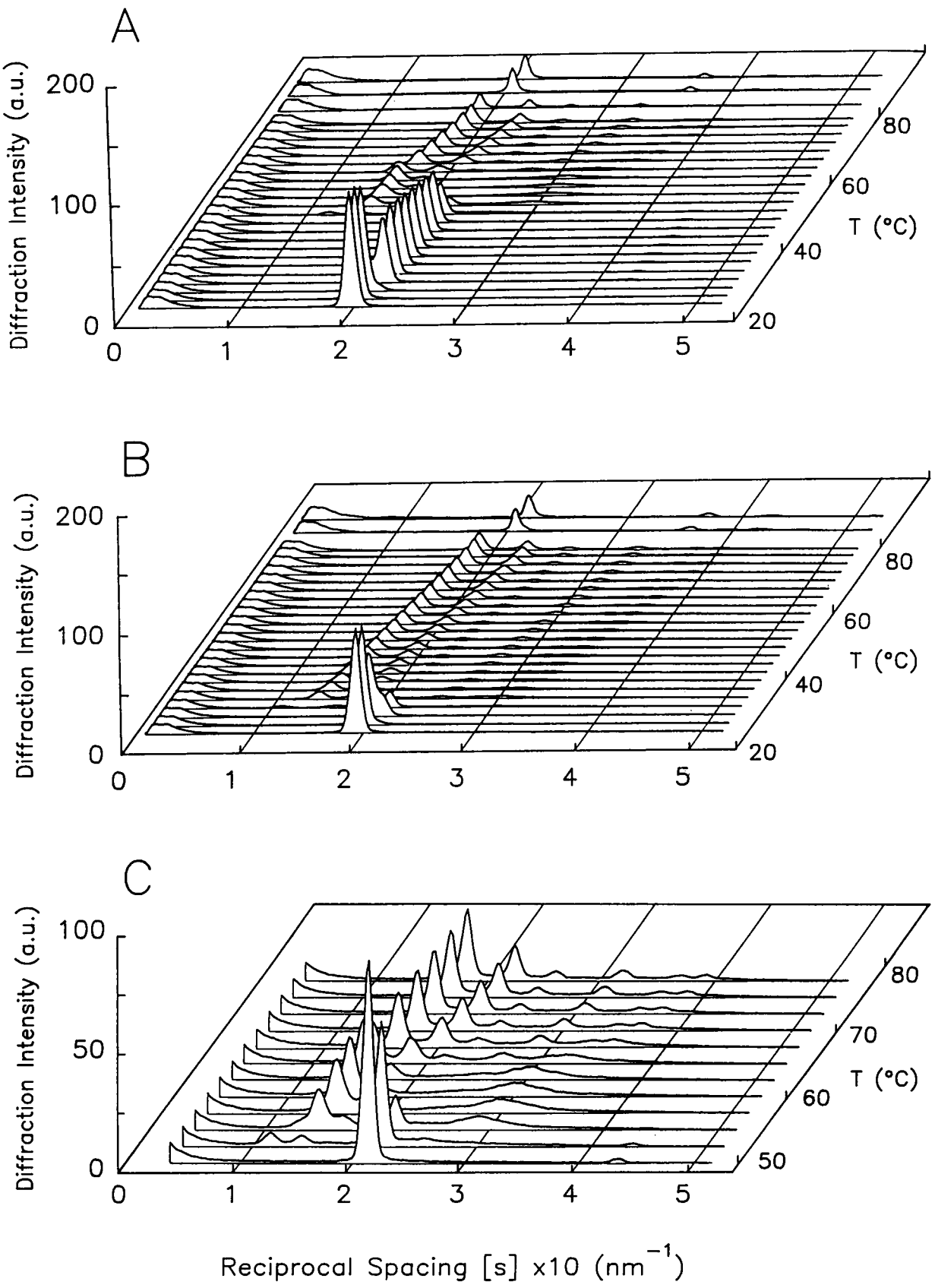

FIGURE 4 Representative x-ray intensity profiles obtained from a sample of the 1,2-di-dodecyl-(β-D-glucopyranosyl)-*rac*-glycerol heated and cooled at 0.5°C · min^{-1} on the synchrotron line at KEK. *A* is a complete heating sequence; *B* is a cooling sequence concentrating on the liquid-crystalline region. *C* is a ×5 magnification of *A* concentrating on the L_α/Q_{II} region. Exposure times were typically of the order of 30 s.

have been unable to identify. At ~85°C the Pn3m phase converts to an H_{II} phase.

The results of the corresponding cooling experiment on the diastereomeric mixture are shown in Fig. 4 *B*. The conversion from the H_{II} phase to the Pn3m phase occurs at ~75°C and this phase remains stable to ~30°C (No conversion to the Ia3d phase is observed.). At this temperature, the Pn3m phase is temporarily transformed into a mixed phase consisting of both the L_α and cubic phases, which then undergoes a transition to the L_β phase. Such an interpretation is in complete agreement with the pattern of thermal events seen in our DSC curves (Fig. 2) and in the initial x-ray measurements (Fig. 3) obtained for both the 1,2-*sn* diastereomer and the diastereomeric mixture. Moreover, the similarity in the heating and cooling measurements of the cubic phase region of the 2,3-*sn* diastereomer may reflect the presence of only a single cubic phase in this sample alone, suggesting that the patterns of nonlamellar as well as gel-phase polymorphism may be significantly affected by the chirality of the glycerol molecule. On the basis of these x-ray diffraction measurements, the minor thermal events seen in the DSC heating thermograms of the 1,2-*sn* compound and the mixture of diastereomers can be identified as L_α/Ia3d, Ia3d/Pn3m, and Pn3m/H_{II}, and those of the 2,3-*sn* compound as L_α/Pn3m and Pn3m/H_{II} phase transitions.

TABLE 2 X-ray diffraction first-order parameters (nm) for the L_β and L_α phases of some diacyl and dialkyl glycerolipids differing in their headgroup structure and the chirality of their glycerol backbone

Lipid species/Chirality	Phase assignment L_β	Phase assignment L_α
DD-β-GlcDAG		
1,2-*sn*	5.0	4.6
2,3-*sn*	5.0	4.6
1,2-*rac*	5.0	4.6
DM-Glycolipids		
1,2-β-Glc [40]	5.4	5.0
1,2-β-Gal [43]	5.5	5.0
1,2-α-Glc [41]	5.4	5.0
DPPE		
1,2-*sn* [14]	6.0	5.0
1,2-*rac* [14]	6.0	5.0
DPPC		
1,2-*sn* [70]	6.4	6.7
1,2-*rac* [71]	6.5	6.7
DiMe-DHPE		
1,2-*sn* [J. Seddon, Pers. comm.]	6.5*	6.6*
	6.5‡	5.6‡
1,2-*rac* [J. Hogan, Pers. comm.]	6.6‡	5.6‡

* Measured in excess water at 30°C (L_β) and 60°C (L_α), respectively.
‡ These samples contained 5 water molecules per lipid molecule at 60°C (L_β) and 80°C (L_α), respectively.

DISCUSSION

Effects of stereochemistry and glycerol chirality on the L_β/L_α phase transition. The DSC and x-ray diffraction measurements reported here show that both β-GlcDAGs and their diastereomeric mixture exhibit L_β/L_α, L_α/Q_{II}, and Q_{II}/H_{II} phase transitions. Changing the chirality of the glycerol molecule does not significantly alter the L_β/L_α phase transition temperature (Table 1) or the magnitude of the first-order spacings of the L_β and L_α phases (Fig. 3, Table 2). Likewise, changing the orientation of the OH4 of the sugar ring from equatorial to axial produces the corresponding β-GalDAGs with L_β/L_α T_m's similar to those of the β-GlcDAGs (33, 50) (Table 1). A comparison of the thermodynamic and x-ray diffraction data obtained for several phospholipid stereoisomers (Tables 1 and 2) shows that neither the chain-melting phase transition or the dimensions of the L_β and L_α phases depend significantly on the chirality of the glycerol backbone. In this respect it is interesting to compare the measurements obtained here for the diastereomeric β-GlcDAGs (Table 1 and Figs. 2–4) with those reported for the 1,2-di-myristoyl-3-*O*-(β-D-glucopyranosyl)-(40), -(α-D-glucopyranosyl)-(41, 42) and -(β-D-galactopyranosyl)-*sn*-glycerols (43). These three molecules differ slightly in their respective L_β/L_α phase transition temperatures but all have first-order spacings that are similar to one another in the L_β and L_α phases. These observations suggest that the structure and dimensions of both the L_β and L_α phases within the dialkyl or diacyl glyceroglycolipids are independent of headgroup orientation/stereochemistry, and that these factors exert only a small influence on the stability of the L_β phase, and hence on the L_β/L_α phase transition temperature. This implies that the differences in stereochemistry and the extent of the steric interactions in the interfacial region of the L_β and L_α phases of these lipid molecules are masked by a combination of interfacial hydration and motional averaging about the molecules' long axis, in agreement with the observations of Seddon et al. (27). However, the chirality of the glycerol molecule does alter the pattern of both the solid state and lamellar/nonlamellar phase behavior in these β-GlcDAGs.

Effects of stereochemistry and glycerol chirality on the formation of L_c phases. In the glucolipids studied here an L_c type phase is observed only in the 1,2-*sn* stereoisomer (Figs. 2 and 3). Changing the orientation of the OH4 of the sugar ring from equatorial to axial produces the corresponding β-GalDAGs. Interestingly, the L_β phases of the diastereomeric β-GalDAGs and their mixture convert to the L_c phase at different rates and the transitions involving the L_c phase occur at different temperatures (Table 1). There have been many reports of differences in solid-state polymorphism of both the chiral and racemic phospholipids on changing the lipid headgroup. Such disparities in the gel-phase behavior have been reported for the L- and DL-DPPCs and DPPEs, and the diastereomeric forms of DPPG and

some PSs (see Table 1). Within each of these lipid groups the chain-melting phase transition temperatures are very similar, whereas the temperatures of transitions involving solid-state transformations, if multiple gel phases are formed, vary significantly with the lipid headgroup and the chirality of the backbone molecule. For example, although the subgel phases of L-DPPC have been extensively investigated (2, 5–8), it is still not clear whether such phases exist in the racemic mixture (6, 7), and this is also true of the DPPGs (51, 52). However, with the L- and DL-DPPEs, while the L_c/L_α phase transition temperatures are very different (66°C versus 82°C, respectively), the first-order spacings for the L_c phases are similar, showing only slight differences in the packing of their hydrocarbon chains (14). In contrast, the D- and L-forms of PS are known to produce different crystalline polymorphs (53). These observations suggest that the kinetic and thermodynamic barriers, which exist at the formation L_c phases, vary with the chemical nature headgroup and that in some cases these barriers are so large that no L_c phase is formed.

From the above examples it is evident that there are underlying differences in the solid-state behavior of the chiral and racemic glycerophospholipids, the bases of which are not well understood. Tenchov and co-workers explained the solid-state behavior of the chiral and racemic PCs and PEs in terms of interactions between DD, LL, and DL pairs of molecules (7, 13). Their explanation assumes that the minimum energy conformations in the D, L, and DL configurations are the same and does not fully describe the nature of the interactions in the interfacial region. Hauser and co-workers (54) have shown that although the conformation of the glycerol backbone of all of the glycerolipids studied is essentially similar, changes in the chemical structure of the headgroup, the acyl chains, the lipid concentration, and the phase state of the lipid usually result in small but significant differences in the rotamer population about the C1–C2 bond of the glycerol moiety. In the L_β or L_c phase, one or two rotamer conformations may dominate, whereas in the L_α phase or in dilute solution there is a rapid exchange between at least three local minimum energy conformations. Thus, with lipid molecules which differ either in their headgroup stereochemistry and/or the chirality of their backbone molecule (e.g., the glycolipids studied here), there may be subtle differences in the kinetic and thermodynamic stabilities of the conformers, but such differences are expected to be small and motionally averaged to the extent that they should not significantly alter the L_β/L_α phase transition temperature or enthalpy (see data listed in Table 1). However, the effects of the aforementioned stereochemical differences should become apparent when the molecule is either conformationally restricted and an L_c-type phase is formed, or when the nature of the molecular assembly changes, such as at the lamellar/nonlamellar phase transition.

In this regard, Bruzik (26), on the basis of NMR spectroscopy measurements, recently suggested that the differences in the pattern of solid-state polymorphism exhibited by the D-*erythro*- and L-*threo*-sphingomyelin (25) could be explained in terms of a difference in the conformation of the C1-C2 bond in the sphingosine backbone. The conformation of the C1–C2 bond in the D diastereomer, which readily forms L_c phases on annealing, is − (minus) synclinal, analogous to the conformation of the crystalline galactosylceramide (55). In contrast, the L diastereomer, which does not readily form L_c phases, shows unrestricted rotation about the C1–C2 bond.

In order to examine the likely effects of changing the glycerol chirality on the molecular conformation of the glycolipids studied here, we constructed space-filling models of the two diastereomeric β-GlcDAGs in which the all-*trans* configuration of the alkyl chain is continuous with that of the glycerol backbone (Fig. 5). It is immediately apparent on close inspection of these models that the relative positions of the ring, glycosidic, and glycerol oxygen atoms change with respect to the *sn*-2 alkyl chain in the two diastereomers and, as a consequence, there are small differences in the interfacial geometry. Nevertheless, the overall shape of the molecules is similar over a range of headgroup conformations, as seen by comparing (Fig. 5, *A* and *B*). This may explain the similarity in the L_β/L_α phase transitions in the three β-GlcDAG samples studied here (Table 1). However, on rotation about the glycerol C2–C3 bond in the 1,2-*sn*-β-GlcDAG diastereomer, two headgroup conformations become visible, one which is only slightly tilted from the vertical (not shown) and another which is highly tilted. In the highly tilted conformation (Fig. 5 *C*), the hydrophobic β surface of the sugar points out towards the aqueous phase, resulting in a conformation similar to the so-called "shovel" shape seen in the crystallographic studies of galactosylceramide (55, 56) and in the molecular dynamics calculations for the corresponding glucosylceramide (57). Although a comparable conformation can be adopted in the corresponding 2,3-*sn* diastereomer, it is only possible if the hydrophilic α surface of the headgroup is exposed to the aqueous environment (Fig. 5 *D*) and, as this structure is sterically hindered, such a conformation may not be energetically favored. Thus, while these minor differences in stereochemistry between the 1,2- and 2,3-*sn* diastereomers may not be sufficient to radically alter the area per molecule, the interfacial hydration in the gel phase, and consequently the L_β/L_α phase transition, they may result in different minimum energy conformations in the 1,2- and 2,3-*sn* compounds, which in turn determine whether or not formation of an L_c phase is favored.

It is widely accepted that molecular conformation is only one of the interactive processes that determine the gross structure and properties of the lipid molecular as-

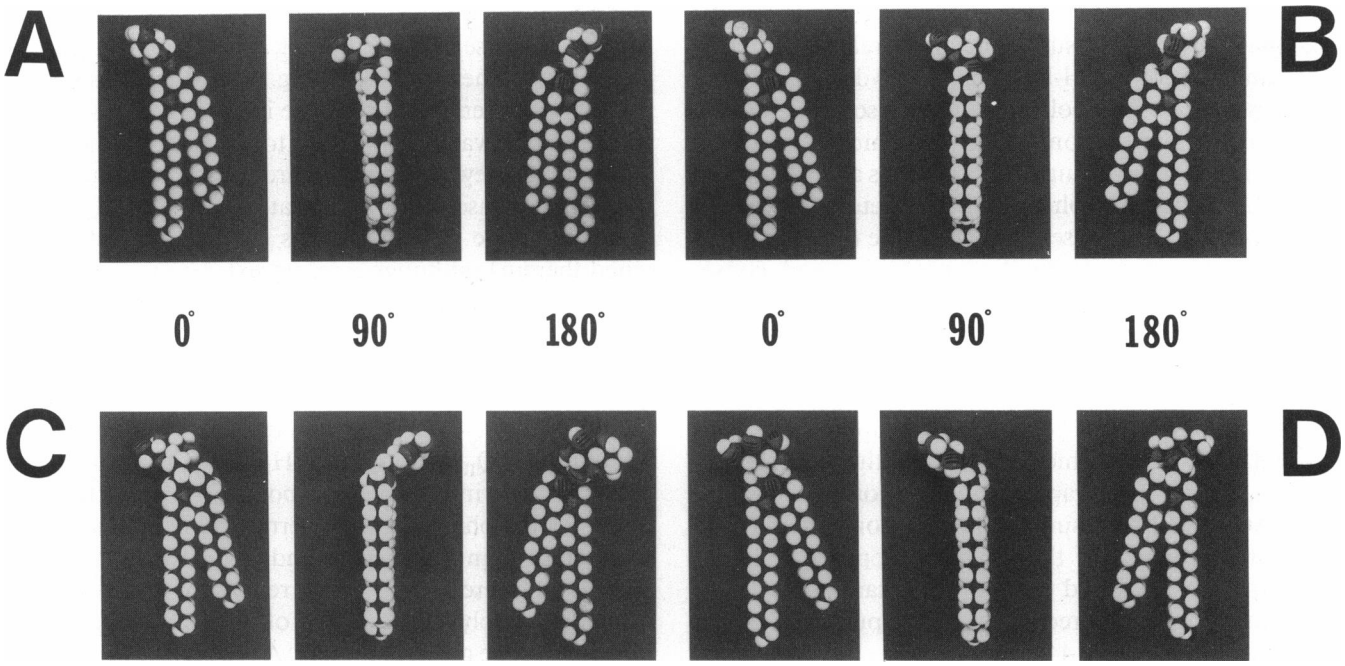

FIGURE 5 Photographs of the space-filling models of the 1,2- and 2,3-Di-*O*-alkyl-1-*O*-(β-D-glucopyranosyl)-*sn*-glycerols. (*A*) 1,2-*sn* diastereomer in which the 1-*O*-alkyl chain and the glycerol molecule are all-*trans*. (*B*) 2,3-*sn* diastereomer in which the 3-*O*-alkyl chain and the glycerol molecule are all-*trans*. (*C*) 1,2-*sn* diastereomer in which the head group conformation is tilted. (*D*) 2,3-*sn* diastereomer in which the head group conformation is tilted. The three photographs in each panel represent 0°, 90°, and 180° views, respectively. See text for further details.

sembly. Indeed, the formation of L_c phases is known to be favored by low hydration (10, 11). It has been suggested that such phases are characterized by strong lipid–lipid intermolecular hydrogen bonds and resemble those seen in x-ray diffraction studies of single crystals (For a review of H-bonding in lipids, see reference 19.) These hydration/dehydration phenomena are known to be determined by the nature of the chemical substituents within the interfacial region (58). Unfortunately, direct dynamic measurements of these solute–solute, solute–solvent H-bonding interactions in water are made almost impossible by the amphipathic nature of lipid molecules and by their tendency to self-assemble. Nevertheless, there is circumstantial evidence in the literature that suggests that there is a correlation between molecular conformation and the H-bonding properties of a lipid molecule that are relevant to our discussion of the data obtained here for the diastereomeric glycolipids and their mixtures. In this respect, Nyholm et al. (56) recently compared the crystal structures of the β-D-galactosylceramide and its permethylated derivative and suggested that the different H-bonding abilities of the headgroup were in part responsible for the differences in headgroup conformation and that such differences might also affect headgroup hydration. This is supported by the work of Kano et al. (59), who observed that the compression of monolayers of octadecyl-α-D-glucopyranoside spread at the air/water interface was different from that of derivatives that differed in their ability to accept and donate H-bonds. In our β-GlcDAGs, we suggest that only the interactions between 1,2-*sn* stereoisomers result in the loss of water from the interfacial region with subsequent formation of an L_c phase.

On the basis of the above observations, we conclude that the headgroup stereochemistry/orientation in the 1,2-*sn* diastereomer is more favorable to the formation of stronger or more extensive H-bonding networks across the bilayer surface than with water, whereas the interfacial geometry of both the 2,3-*sn*-β-GlcDAGs and the diastereomeric mixture is more favorable to the formation of H-bonds with water. This is supported by the observation that the rate of L_β/L_c phase conversion in the β-GalDAGs decreases in the order 1,2-*sn* > mixture > 2,3-*sn* (Mannock, D., unpublished experiments). Such an interpretation is consistent with our own measurements on the 1,2-*sn*-glycosyl diacylglycerols (40, 41, 43) and those of Hinz's group on the 1,2-*sn*-glucosyl and galactosyl dialkylglycerols (28, 29, 33, 50), which show that both the structure of the L_c phase and the kinetics of the L_β/L_c conversion process are dependent on headgroup stereochemistry. Additional support for this argument has recently been provided by the observation that the binding of aldohexoses and aldopentoses to a resorcinol–dodecanal cyclotetramer at the air–water interface is determined by the stereochemistry of the carbohydrate molecule and its hydrogen-bonding properties (60, 61). Thus, in the glycosyl glycerides, a small difference in the stereochemistry of the headgroup or interfacial region

may determine the headgroup orientation (See, for example, the ^{2}H-NMR measurements of Jarrell's group (30–32).) and thereby the H-bonding and hydration characteristics of the entire polar region, and so influence the molecular conformation of the lipid molecule over a wide range of temperature. Such changes alter the stability of the hydration sphere and thus determine the kinetics of the L_β/L_c phase conversion, the formation and strength of surface H-bonding networks, and consequently the pattern and energetics of L_c-phase transitions in these diastereomers, as well as in other amphiphilic lipid molecules. This suggestion is supported by x-ray diffraction, DSC, and differential scanning densitometry measurements on the 1,2-*sn*-β-GlcDAGs and -β-GalDAGs (50), which show that the β-GalDAGs form L_c phases more rapidly than the corresponding β-GlcDAGs. Such measurements also confirm that the greatest divergence in the physical properties of lipid isomers is to be found in phases containing the least amount of water, in agreement with the published observations (6, 13, 14, 28, 44).

Effects of stereochemistry and glycerol chirality on the lamellar/nonlamellar phase transitions. Changing the stereochemistry of the sugar headgroup from β-Glc to β-Gal does not significantly alter the L_β/L_α phase transition temperature (Table 1), suggesting that headgroup conformation and hydration in these two glycosyl dialkyl glycerols are similar, contrary to one recent suggestion (50). However, the L_α/H_{II} phase transition temperature in the di-14:0-β-GalDAGs is significantly higher than that in the di-14:0-β-GlcDAGs (63–65°C versus 56–58°C). The chirality of the glycerol backbone also affects the lamellar/nonlamellar phase behavior in these β-GlcDAGs. The L_α/Q_{II} and Q_{II}/H_{II} phase transitions occur at higher temperatures in the 1,2-*sn* compound and the diastereomeric mixture than in the 2,3-*sn* diastereomer (Figs. 2 and 3, Table 1). This effect is chain-length dependent, since there is no difference in the L_α/H_{II} phase transitions of the corresponding di-14:0-β-GlcDAGs or β-GalDAGs (Table 1). The most likely explanation for this behavior is that the hydrocarbon chain interactions dominate the lipid physical properties at longer chain lengths, thus reducing the influence of the substituents in the interfacial region.

In the di-12:0-β-GlcDAGs, all three samples possess an inverted cubic phase, the dimensions of which are not affected by the chirality of the backbone (Fig. 3) and which are consistent with the Pn3m/Pn3 lattice. At higher temperatures in all three lipid samples, the Q_{II} phase is replaced by an H_{II} phase. At lower temperatures in the cubic phase region of both the 1,2-*sn* compound and the diastereomeric mixture, an additional cubic phase is observed that is consistent with an Ia3d lattice; this lattice has also been reported with other lipids (27). The existence of both an L_α/Q_{II} and Q_{II}/H_{II} phase transition in the 1,2-*sn*-di-12:0-β-GlcDAGs has recently been confirmed (50). The cell lattice parameter (**a**) of this cubic phase is larger in the 1,2-*sn* compound than in the diastereomeric mixture (Fig. 3) and may also occur over a wider temperature range in the former, although such an observation is difficult to verify experimentally.

Relatively few amphiphiles are known to form multiple cubic phases in excess water (16, 27). The best known are the monoglycerides (48, 62 and references cited therein), although a recent extension of the phase diagram of DDPE (10, 11, 27) has shown the existence of both the Im3m and Pn3m cubic phases between ~90 and 135°C, below the transition to the H_{II} phase. Our previous studies of both the dialkyl and diacyl glycolipids (38, 39, 41, 44) have shown that it is not uncommon for multiple Q_{II} phases and a H_{II} phase to be observed below 100°C in a single compound (44) and that the Pn3m cubic phase is the preferred cubic phase at high temperatures in these compounds ($N < 13$). As far as we are aware, there have been no reports of changes in the nonlamellar phase properties of PEs on changing the chirality of the glycerol moiety. A recent x-ray investigation of both L- and DL-di-methyl-DHPE at low water content showed that molecular chirality has no effect on the structure of the cubic phase formed (27), although no data on the effect of temperature and hydration on the temperature range of this cubic phase in these two compounds was presented. Indeed, because PEs have only a single chiral center, the difference between the lamellar/nonlamellar phase transitions of L- and DL-PEs may be quite small.

Shyamsunder et al. (16) have observed highly stable Pn3m/Pn3 structures in dioleoylphosphatidylethanolamine (DOPE) dispersed in excess water upon repeated cycling across the L_α/H_{II} transition. Although many diffracted orders were observed that were consistent with a Pn3m/Pn3 lattice, the unit cell size and the transition temperature was, by nature of the method, difficult to determine. It was suggested that the formation of these cubic structures is kinetically hindered by formation energies. It is still not known if the cubic structures observed with DOPE are stable equilibrium phases or metastable phases. Moreover, the difficulty in forming and observing cubic phases appears not to be confined to DOPE, but rather seems characteristic of many highly water-insoluble lipid systems. Following (16), we speculate that highly water-insoluble lipids present large formation barriers to any phase that involves changes in interfacial topology and, thus, rips the interfacial surface. This leads to structures whose formation and lattice size are very dependent on the history of the sample. What does appear clear, however, is that whenever cubic phases are observed in excess water systems, they appear at temperatures intermediate to lamellar and H_{II} phases.

Why the transition proceeds directly from the L_α phase to the Pn3m cubic phase in the 2,3-*sn*-β-GlcDAG, rather than via the Ia3d phase seen in the 1,2-*sn* and diastereomeric mixture, is not clear. The Ia3d cubic

phase intermediate observed in the 1,2-*sn* form en route to the Pn3m phase has been found at low hydration levels in PEs, whereas in excess water this phase is replaced by the Im3m cubic phase (11, 27). We have not seen the Im3m cubic phase in any of the glycolipids studied here (however, see reference 43) and it is interesting to speculate that these differences in the cubic phase regions of DDPE and DD-β-GlcDAG may reflect differences in the headgroup hydration of these two lipids.

It is interesting to consider the similarities in the dimensions of the L_β and L_α phases and the T_m's of the L_β/L_α phase transitions of the glycolipids and phospholipids listed in Tables 1 and 2, which suggest that the steric interactions in the interfacial region are masked in excess water. If this assumption is valid, it is difficult to rationalize their disparate lamellar/nonlamellar phase transitions (Fig. 2 and Table 1) and to envisage the driving forces responsible for these differences. The higher L_α/H_{II} phase transition temperatures of the PEs relative to those of the glycolipids do not correlate with the slightly larger molecular area measured in the liquid-condensed phase (4.1 nm versus 4.0 nm) for monolayers of the di-16:0acyl-β-GlcDG (63). However, those measurements were made at the same temperature relative to the L_β/L_α phase transitions in each lipid and as such may not be representative of the molecular area at higher temperatures just below the L_α/H_{II} phase transitions. Indeed, our previous work suggests that the glucose headgroup may actually occupy a smaller area at high temperatures than does the phosphorylethanolamine headgroup (63). This idea is supported by the observation that the rotational motion of the sugar headgroup is slower in the L_α phase than the equivalent PE headgroup (30, 64), and by the observation that the headgroup hydration in the H_{II} phase is lower for a β-GalDG (5.3 H_2O/mol) than for the corresponding PE (7.9 H_2O/mol) (65). This is further supported by our own recent x-ray measurements of the *rac*-di-12:0-β-GlcDAG (47).

It is more difficult to understand why two lipid molecules with sterically and chemically similar headgroups should differ in their phase behavior. The dialkyl- and diacyl β-D-glucosyl- and β-galactosyl-*sn*-glycerols can be considered as one example, and the diastereomers of the di-dodecyl-β-GlcDAGs as another (see Table 1). In either case, within each data set the L_β/L_α phase transition temperatures are very close, yet the lamellar/nonlamellar phase transitions may be significantly different. From our earlier discussions of the molecular models, it is evident that the overall molecular shape is similar in each case (β-Glc versus β-Gal, 1,2-*sn* diastereomer versus 2,3-*sn* diastereomer), but that small differences in molecular geometry and conformation exist. It seems unlikely that these differences themselves would directly change the molecular cross-sectional area and consequently the lamellar/nonlamellar phase transitions. A more probable explanation is that the L_α/H_{II} phase transition is considerably more sensitive to small changes in headgroup and interfacial hydration than is the L_β/L_α phase transition. This argument is strengthened by the observation that substituting D_2O for H_2O lowers the L_α/H_{II} phase transition temperature of some diacyl-PEs more than it raises their L_β/L_α phase transition temperature (66). In this respect, it seems reasonable to suggest that in the glycolipids studied here, small changes in headgroup stereochemistry may alter the interfacial hydration and by so doing regulate the lamellar/nonlamellar phase transition. We suggest that the temperature at which a glycolipid dispersed in excess water forms a nonlamellar phase is determined primarily by the orientation and stereochemistry (and hence conformation) of the carbohydrate headgroup, as discussed in the previous section, and the extent to which the surrounding water molecules are ordered or disordered (67). In this way, the dynamic volume of the headgroup/interfacial region will be determined by a combination of the strength of these headgroup-solvent H-bonding interactions and the release of bound water to the bulk phase with increasing temperature, rather than the size of the headgroup per se. If this argument is valid, then the differences in the pattern of phase behavior between the two diastereomers may reflect the sum of the small differences in headgroup conformation plus the more significant differences in "hydration" properties, which are moderated by opposing contributions from the hydrocarbon chains. Thus, the presence of the Ia3d phase in the 1,2-*sn* isomer and the diastereomeric mixture may represent a compromise either in terms of curvature or chain packing between the L_α bilayer and the Pn3m phase (47). Such ideas are consistent both with the geometric concepts of Israelachvili et al. (68) and with the curvature hypotheses of Rand and co-workers (69), since they are likely to effect both the molecular cross-sectional area (a_0) and the depth of the pivotal plane in the interfacial region of the molecule.

These arguments suggest that lamellar/nonlamellar phase transitions may be regulated in the lipid interfacial region by many factors. The most visible contributions originate from the steric and chemical properties of the lipid headgroup itself. But the bulk properties of the solvent, the strength of H-bonding interactions with the solvent, and consequently the temperature-dependent stability of the "hydration" sphere in the interfacial region of the lipid, are also of great significance. Our own studies also suggest that the dimensionless packing parameter (v/a_0l_c) (68) is only useful when comparing lipids with headgroups which differ greatly in size, for example, glucosyl, maltosyl, maltotriosyl (50). A comparison of lipid headgroups of similar size, as in this study, suggests that this parameter is too coarse to be of much use. Instead, it might be more prudent to consider the lipid interfacial region in terms of solute–solute and solvent–solute interactions and more accurate to describe the shape of a lipid molecule in terms of a solvated headgroup partial molal volume which is counterbalanced by

that of the hydrocarbon chains, since it is a combination of both of these factors that regulate membrane curvature (69).

While it is evident that there are many more contributions from the headgroup/interfacial regions and their interactions with water that determine the phase properties of amphiphilic lipid molecules than had hitherto been envisaged, at the present time our understanding of these factors is hindered by our difficulties in measuring them. Whether the differences in both gel-phase and nonlamellar-phase polymorphism between the 1,2-*sn*-β-GlcDAG and 2,3-*sn*-β-GlcDAG studied here have any biological implications is not clear. It is possible that organisms containing dialkyl glycosyl glycerols, such as the Archaebacteria, prefer the 2,3-*sn* diastereomers because of the factors which cause dispersions of the 2,3-*sn* lipids to form nonlamellar structures more readily than the 1,2-*sn* compounds. However, for the moment such a statement must await further investigations on a wider range of dialkyl glycolipids.

We would like to thank Drs. John Seddon and Jacqueline Hogan for providing us with preprints of their work prior to publication and for allowing us to present their unpublished x-ray diffraction measurements of the dimethyl-DHPEs.

This work was supported by operating and major equipment grants from the Medical Research Council of Canada and the Alberta Heritage Foundation for Medical Research to R. N. McElhaney, by NIH grant GM-32614 and DOE grant DE-FG02-87ER60522 to S. M. Gruner, and by the National Laboratory for High Energy Physics (Japan) grant 90-071 to M. Akiyama. D. A. Mannock was supported by an AHFMR Postdoctoral Fellowship. D. C. Turner was supported by an NIH traineeship (Grant 5T32GM07312) and by a Garden State Graduate Fellowship. M. Akiyama was also supported by the University of Alberta-University of Sapporo Medical Scientist exchange program.

Received for publication 12 December 1991 and in final form 20 May 1992.

REFERENCES

1. Lewis, R. N. A. H., B. D. Sykes, and R. N. McElhaney. 1987. Thermotropic phase behaviour of model membranes composed of phosphatidylcholines containing dl-methyl anteisobranched fatty acids: 1. Differential scanning calorimetric and 31P-NMR spectroscopic studies. *Biochemistry.* 26:4036–4044.
2. Lewis, R. N. A. H., N. Mak, and R. N. McElhaney. 1987. Differential scanning calorimetric study of the thermotropic phase behavior of model membranes composed of phosphatidylcholines containing linear saturated fatty acyl chains. *Biochemistry.* 26:6118–6126.
3. Lewis, R. N. A. H., B. D. Sykes, and R. N. McElhaney. 1988. Thermotropic phase behaviour of model membranes composed of phosphatidylcholines containing cis-monounsaturated acyl chain homologues of oleic acid. Differential scanning calorimetric and 31P-NMR spectroscopic studies. *Biochemistry.* 27:880–887.
4. Lewis, R. N. A. H., H. H. Mantsch, and R. N. McElhaney. 1989. Thermotropic phase behaviour of phosphatidylcholines with ω-tertiary-butyl fatty acyl chains. *Biophys. J.* 56:183–193.
5. Lipka, G., B. Z. Chowdhry, and J. M. Sturtevant. 1984. A comparison of phase transition properties of 1,2-diacylphosphatidylcholines and 1,2-diacylphosphatidylethanolamines in H_2O and D_2O. *J. Phys. Chem.* 88:5401–5406.
6. Kodama, M., H. Hashigami, and S. Seki. 1985. Static and dynamic calorimetric studies of three kinds of phase transition in the systems of L- and DL-dipalmitoylphosphatidylcholine/water. *Biochim. Biophys. Acta.* 814:300–306.
7. Boyanov, A. I., B. G. Tenchov, R. D. Koynova, and K. Koumanov. 1983. Absence of subtransition in racemic dipalmitoylphosphatidylcholine vesicles. *Biochim. Biophys. Acta.* 732:711–713.
8. Boyanov, A. I., R. D. Koynova, and B. G. Tenchov. 1986. Effect of lipid admixtures on the L-dipalmitoylphosphatidylcholine subtransition. *Chem. Phys. Lipids.* 39:155–163.
9. Seddon, J. M., K. Harlos, and D. Marsh. 1983. Metastability and polymorphism in the gel and fluid bilayer phases of dilauryl-phosphatidylethanolamine. *J. Biol. Chem.* 258:3850–3554.
10. Seddon, J. M., G. Cevc, and D. Marsh. 1983. Calorimetric studies of the gel-fluid (L_β-L_α) and lamellar-inverted hexagonal (L_α-H_{II}) phase transitions in dialkyl- and diacylphosphatidylethanolamines. *Biochemistry.* 22:1280–1289.
11. Seddon, J. M., G. Cevc, R. D. Kaye, and D. Marsh. 1984. X-ray diffraction study of the polymorphism of hydrated diacyl- and dialkylphosphatidylethanolamines. *Biochemistry.* 23:2634–2644.
12. Mantsch, H. H., S. C. Hsi, K. W. Butler, and D. G. Cameron. 1983. Studies on the thermotropic behaviour of aqueous phosphatidylethanolamines. *Biochim. Biophys. Acta.* 728:325–330.
13. Tenchov, B. G., A. I. Boyanov, and R. D. Koynova. 1984. Lyotropic polymorphism of racemic dipalmitoylphosphatidylethanolamine. A Differential Scanning Calorimetry Study. *Biochemistry.* 23:3553–3558.
14. Tenchov, B. G., L. J. Lis, and P. J. Quinn. 1988. Structural rearrangements during crystal–liquid-crystal and gel–liquid-crystal phase transitions in aqueous dispersions of dipalmitoylphosphatidylethanolamine. A time resolved x-ray diffraction study. *Biochim. Biophys. Acta.* 942:305–314.
15. Wilkinson, D. A., and J. F. Nagle. 1981. Dilatometry and calorimetry of saturated phosphatidylethanolamine dispersions. *Biochemistry.* 20:187–192.
16. Shyamsunder, E., S. M. Gruner, M. W. Tate, D. C. Turner, P. T. C. So, and C. P. S. Tilcock. 1988. Observation of inverted cubic phase in hydrated dioleoylphosphatidylethanolamine membranes. *Biochemistry.* 27:2332–2336.
17. Lewis, R. N. A. H., D. A. Mannock, R. N. McElhaney, D. C. Turner, and S. M. Gruner. 1989. The effect of fatty acyl chain length and structure on the lamellar gel to liquid-crystalline and lamellar to reversed hexagonal phase transitions of aqueous phosphatidylethanolamine dispersions. *Biochemistry.* 28:541–548.
18. Hawthorne, J. N., and G. B. Ansell, editors, 1982. Phospholipids. New Comprehensive Biochemistry, Vol. 4. Elsevier Biomedical Press, Amsterdam.
19. Boggs, J. M. 1987. Lipid intermolecular hydrogen bonding: Influence on structural organization and membrane function. *Biochim. Biophys. Acta.* 906:353–404.
20. Sakurai, I., T. Sakurai, T. Seto, and S. Iwayanagi. 1983. Lyotropic phase transitions in single crystals of L- and DL-dipalmitoylglycerophosphocholines. *Chem. Phys. Lipids.* 32:1–11.
21. Dorset, D. L. 1976. Aliphatic chain packing in three crystalline polymorphs of a saturated racemic phosphatidylethanolamine. A quantitative electron diffraction study. *Biochim. Biophys. Acta.* 424:396–403.

22. Boyanov, A., and B. Tenchov. 1985. Phase diagrams of two component lipid membranes. Properties of the phosphatidylcholine subtransition. *Int. Agrophys.* 1:225–232.

23. Tsai, M-D., R.-T. Jiang, and K. Bruzik. 1983. Phospholipids chiral at phosphorus. 4. Could membranes be chiral at phosphorus? *J. Am. Chem. Soc.* 105:2478–2480.

24. Wisner, D. A., T. Rosario-Jansen, and M-D. Tsai. 1983. Phospholipids chiral at phosphorus. Configurational effect on the thermotropic properties of chiral dipalmitoylphosphatidylcholine. *J. Am. Chem. Soc.* 108:8064–8068.

25. Bruzik, K. S. and M. D. Tsai. 1987. A calorimetric study of the thermotropic behavior of pure sphingomyelin diastereomers. *Biochemistry.* 26:5364–5368.

26. Bruzik, K. S. 1988. Conformation of the polar headgroup of sphingomyelin and its analogues. *Biochim. Biophys. Acta.* 939:315–326.

27. Seddon, J. M., J. L. Hogan, N. A. Warrender, and E. Pebay-Peroula. 1990. Structural studies of phospholipid cubic phases. *Progr. Colloid Polym. Sci.* 81:189–197.

28. Hinz, H.-J., L. Six, K.-P. Reuss, and M. Liefländer. 1985. Headgroup contributions to bilayer stability: Monolayer and calorimetric studies on synthetic, stereochemically uniform glucolipids. *Biochemistry.* 24:806–813.

29. Koynova, R. D., H. L. Kuttenreich, B. G. Tenchov, and H.-J. Hinz. 1988. Influence of head-group interactions on the miscibility of synthetic stereochemically pure glycolipids and phospholipids. *Biochemistry.* 27:4612–4619.

30. Jarrell, H. C., A. J. Wand, J. B. Giziewicz, and I. C. P. Smith. 1987. The dependence of glyceroglycolipid orientation and dynamics on head-group structure. *Biochim. Biophys. Acta.* 897:69–82.

31. Auger, M., and H. C. Jarrell. 1990. Elucidation of slow motions in glycoglycerolipid bilayers by two-dimensional solid state deuteron NMR. *Chem. Phys. Lett.* 165:162–167.

32. Auger, M., D. Carrier, I. C. P. Smith, and H. C. Jarrell. 1990. Elucidation of motional modes in glycoglycerolipid bilayers. A ^{2}H NMR relaxation and lineshape study. *J. Am. Chem. Soc.* 112:1373–1381.

33. Kuttenreich, H., H-J. Hinz, M. Inczedy-Marcsek, R. Koynova, B. Tenchov, and P. Laggner. 1988. Polymorphism of synthetic 1,2-dialkyl-3-O-β-D-Galactosyl-*sn*-glycerols of different chain lengths. *Chem. Phys. Lipids.* 47:245–260.

34. Endo, T., K. Inoue, and S. Nojima. 1982. Physical properties and barrier functions of synthetic glyceroglycolipids. *J. Biochem.* 92:953–960.

35. Endo, T., K. Inoue, S. Nojima, T. Sekiya, K. Ohki, and Y. Nozawa. 1983. Electron microscopic study on the structures formed by mixtures containing synthetic glyceroglycolipids. *J. Biochem.* 93:1–6.

36. Ratledge, C., and S. G. Wilkinson, editors. 1988. Microbial Lipids, Vol. 1. Academic Press. New York.

37. Quinn, P. J., and W. P. Williams. 1983. The structural role of lipids in photosynthetic membranes. *Biochim. Biophys. Acta.* 737:223–226.

38. Mannock, D. A., R. N. A. H. Lewis, and R. N. McElhaney. 1987. An improved procedure for the preparation of 1,2-di-O-acyl-3-O-(β-D-glucopyranosyl)-*sn*-glycerols. *Chem. Phys. Lipids.* 43:113–127.

39. Mannock, D. A., R. N. A. H. Lewis, and R. N. McElhaney. 1990. The chemical synthesis and physical characterization of 1,2-di-O-Acyl-3-O-(α-D-Glucopyranosyl)-*sn*-glycerols, an important class of membrane glycolipids. *Chem. Phys. Lipids.* 55:309–321.

40. Mannock, D. A., R. N. A. H. Lewis, A. Sen, and R. N. McElhaney. 1988. The physical properties of glycosyl diacylglycerols. Calorimetric studies of a homologous series of 1,2-Di-O-acyl-3-O-(β-D-Glucopyranosyl)-*sn*-glycerols. *Biochemistry.* 27:6852–6859.

41. Mannock, D. A., R. N. A. H. Lewis, and R. N. McElhaney. 1990. The physical properties of glycosyl diacylglycerols. 1. Calorimetric studies of a homologous series of 1,2-Di-O-acyl-3-O(α-D-Glucopyranosyl)-*sn*-glycerols. *Biochemistry.* 29:7790–7799.

42. Sen, A., S. W. Hui, D. A. Mannock, R. N. A. H. Lewis, and R. N. McElhaney. 1990. The physical properties of glycosyl diacylglycerols. 2. X-ray diffraction studies of a homologous series of 1,2-diacyl-3-O-(α-D-glucopyranosyl)-*sn*-glycerols. *Biochemistry.* 29:7799–7804.

43. Mannock, D. A., and R. N. McElhaney. 1991. Differential scanning calorimetry and x-ray diffraction studies of a series of synthetic β-D-galactosyl diacylglycerols. *Biochem. Cell Biol.* 69:863–867.

44. Akiyama, M., D. A. Mannock, R. N. A. H. Lewis, and R. N. McElhaney. 1992. Synthesis and thermotropic characterization of a homologous series of dialkyl-β-D-Glucopyranosyl-glycerols. *Chem. Phys. Lipids.* In press.

45. Gruner, S. M., J. R. Milch, and G. T. Reynolds. 1982. A slow scan SIT-TV detector for quantitative recording of weak x-ray diffraction images. *Rev. Sci. Instrum.* 53:1770–1778.

46. Akiyama, M., and Y. Terayama. 1978. Detection of x-ray diffraction pattern by MOS image sensor. *J. Pre-Med. Sapporo Med. Coll.* 19:59–64.

47. Turner, D. C., S. G. Gruner, Z-G. Wang, D. A. Mannock, and R. N. McElhaney. 1992. A structural study of the inverted cubic phases and Gaussian curvature of didodecyl-β-D-glucopyranosyl-*rac*-glycerol. *J. de Physique.* In press.

48. Mariani, P., V. Luzzati, and H. Delacroix. 1988. Cubic phases of lipid-containing systems: Structure analysis and biological implications. *J. Mol. Biol.* 204:165–189.

49. Tate, M. W., and S. G. Gruner. 1989. Temperature dependence of the structural dimensions of the inverted hexagonal (H_{II}) phase of phosphatidylethanolamine-containing membranes. *Biochemistry.* 28:4245–4253.

50. Hinz, H-J., H. Kuttenreich, R. Meyer, M. Renner, R. Frund, R. Koynova, A. I. Boyanov, and B. G. Tenchov. 1991. Stereochemistry and size of sugar headgroups determine structure and phase behaviour of glycolipid membranes: densitometric, calorimetric and x-ray studies. *Biochemistry USA.* 30:5125–5138.

51. Ranck, J. L., T. Keira, and V. Luzzati. 1977. A novel packing of the hydrocarbon chains in lipids. The low temperature phases of dipalmitoylphosphatidylglycerol. *Biochim. Biophys. Acta.* 488:432–441.

52. Ranck, J. L., and J. F. Tocanne. 1982. Choline and acetylcholine induce interdigitation of hydrocarbon chains in dipalmitoylphosphatidylglycerol lamellar phase with stiff chains. FEBS (Fed. Eur. Biochem. Soc.) Lett. 143:171–174.

53. Hauser, H., F. Paltauf, and G. G. Shipley. 1982. Structure and thermotropic phase behavior of phosphatidylserine bilayer membranes. *Biochemistry.* 21:1061–1067.

54. Hauser, H., I. Pascher, and S. Sundell. 1988. Preferred conformation and dynamics of the glycerol backbone in phospholipids. An NMR and x-ray single-crystal analysis. *Biochemistry.* 27:9166–9174.

55. Pascher, I., and S. Sundell. 1977. Molecular arrangements in sphingolipids. The crystal structure of cerebroside. *Chem. Phys. Lipids.* 20:175–191.

56. Nyholm, P-G., I. Pascher, and S. Sundell. 1990. The effect of hydrogen bonds on the conformation of glycosphingolipids. Methylated and unmethylated cerebroside studied by x-ray single crystal analysis and model calculations. *Chem. Phys. Lipids.* 52:1–10.

57. Wynn, C. H., A. Marsden, and B. Robson. 1986. Calculation of

the conformation of glycosphingolipids. 1. β-D-glucosyl-*N*-(2-D-hydroxyoctadecanoyl)-D-dihydrosphingosine (glucosyl-ceramide) and α-D-*N*-acetylneuraminyl-(2→3)-β-D-galactose. *J. Theor. Biol.* 119:81–87.

58. Cevc, G. 1987. How membrane chain melting properties are regulated by the polar surface of the lipid bilayer. *Biochemistry.* 26:6305–6310.
59. Kano, K., T. Ishimura, and S. Hashimoto. 1991. Control of headgroup orientation by glucolipid. *J. Phys. Chem.* 95:7839–7843.
60. Aoyama, Y., Y. Tanaka, and S. Sugahara. 1989. Molecular recognition. 5. Molecular recognition of sugars via hydrogen-bonding interaction with a synthetic polyhydroxy macrocycle. *J. Am. Chem. Soc.* 111:5397–5404.
61. Kurihara, K., K. Ohto, Y. Tanaka, Y. Aoyama, and T. Kunitake. 1991. Molecular recognition of sugars by monolayers of resorcinol-dodecanal cyclotetramer. *J. Am. Chem. Soc.* 113:444–450.
62. Caffrey, M. 1987. Kinetics and mechanism of transitions involving the lamellar, cubic, inverted hexagonal, and fluid isotropic phases of hydrated monoacylglycerides monitored by time-resolved x-ray diffraction. *Biochemistry.* 26:6349–6363.
63. Ashgarian, B., D. A. Cadenhead, D. A. Mannock, R. N. A. H. Lewis, and R. N. McElhaney. 1989. A comparative monomolecular film study of 1,2-di-O-palmitoyl-3-O-(α- and β-D-glucopyranosyl)-*sn*-glycerols. *Biochemistry.* 28:7102–7106.
64. Browning, J. L. 1981. Motions and interactions of phospholipid headgroups at the membrane surface. 3. Dynamic properties of amine containing headgroups. *Biochemistry.* 20:7144–7155.
65. Sen, A. and S-W. Hui. 1988. Direct measurement of headgroup hydration of polar lipids in inverted micelles. *Chem. Phys. Lipids.* 49:179–184.
66. Epand, R. M. 1990. Hydrogen bonding and the thermotropic transitions of phosphatidylethanolamines. *Chem. Phys. Lipids.* 52:227–230.
67. Suggett, A. 1975. *In* Water, A Comprehensive Treatise, Vol. 4. F. Franks, editor. Plenum Press, New York.
68. Israelachvili, J. N., S. Marčelja, and R. G. Horn. 1980. Physical principles of membrane organization. *Quart. Rev. Biophys.* 13:121.
69. Rand, R. P., N. L. Fuller, S. M. Gruner, and V. A. Parsegian. 1990. Membrane curvature, lipid segregation and structural transitions for phospholipids under dual-solvent stress. *Biochemistry.* 29:76–87.
70. Lis, L. J., M. McAlister, N. Fuller, R. P. Rand, and V. A. Parsegian. 1982. Interactions between neutral phospholipid bilayer membranes. *Biophys. J.* 37:657–666.
71. Inoko, Y., and T. Mitsui. 1978. Structural parameters of dipalmitoyl phosphatidylcholine lamellar phases and bilayer phase transitions. *J. Phys. Soc. Jpn.* 44:1918–1924.